

## Thermodynamic Properties of Nonideal Gases. II. The Strongly Ionized Gas\*

H. C. Graboske, Jr., D. J. Harwood, and H. E. DeWitt

*Lawrence Radiation Laboratory, University of California, Livermore, California 94550*

(Received 18 September 1970)

The thermodynamic equilibrium properties of strongly ionized multicomponent gas mixtures are investigated by application of the free-energy minimization method. For high-temperature regions where the Coulomb interaction is the dominant perturbation, the many-body partition function is developed from quantum cluster-expansion theory. The Coulomb free energy is given as the sum of the first- and second-order direct-interaction terms, plus the first three exchange-interaction terms. All five terms are exact in the classical limit, i. e., where Maxwell-Boltzmann statistics apply. The direct terms are correct for weak electron degeneracy and include wave-mechanical effects, while the first-order exchange term is exact for all degrees of degeneracy. The theoretical model is applied to multicomponent mixtures of hydrogen and of helium in the temperature range 50–2000 eV. The combination of the ring term plus higher-order terms significantly extends the region of applicability of the model over a classical electrostatic model. Specifically, electron degeneracy, the short-range cut-off in the ring term, and the three-rung ladder (second-order direct) term all operate to produce much less divergent thermodynamic results at a given density and temperature. First-order exchange is important even at moderate values of the electron-degeneracy parameter. The thermodynamic results indicate that evaluation of the exact quantum-mechanical ring term is essential for wider application of the perturbation-expansion theory, as is the development of a second-order exchange term for arbitrary degeneracy.

### I. INTRODUCTION

The thermodynamic properties of nonideal multicomponent gas mixtures require numerous interaction effects to describe adequately the many-body system over wide ranges of density and temperature. In this paper, the free-energy minimization method, described in Paper I,<sup>1</sup> is used to study a systematic treatment of the many-body partition function of the strongly ionized gas. By limiting our attention to the strongly ionized gas and the Coulomb interactions, a detailed analysis of these effects can be made which is relatively independent of the other internal and configurational interactions.

The quantum statistical mechanics of dense ionized gases has been studied intensively over the past ten years,<sup>2–6</sup> and numerous theoretical developments have appeared which can significantly improve the calculation of thermodynamic equilibrium compositions and properties of strongly ionized gases. The quantum perturbation expansion and its associated diagram techniques provide a quantum-dynamic generalization of the classical electrostatic model of plasmas, one in which the theoretical partition function can be expressed as a series of direct and exchange terms in the screened Coulomb interaction. Although the perturbation-expansion theory is difficult and has complex analytical features, it can be handled by straightforward numerical methods. The perturbation expansion as utilized here consists of the

first- and second-order direct interaction terms plus first-, second-, and third-order exchange interactions. The numerical studies have yielded an exact solution for the first-order exchange term for electrons, valid for all degrees of degeneracy. The other terms are presently available as approximations, exact only in the specified asymptotic limits. However, their range of validity has been extended over the previously available region of phase space.

In Secs. II–VI, we present a brief discussion of the many-body perturbation expansion and a detailed description of the various Coulomb-interaction free-energy terms. Next, a series of numerical models are constructed which demonstrate the effects of the various terms, both on the equilibrium configuration and on the thermodynamic properties. The region of density-temperature space studied is restricted to high temperatures, where the gas is strongly ionized and where competing nonideal effects, specifically the confined atom bound-state perturbation and the excluded volume configurational terms, are small. The hydrogen plasma is chosen for analysis, but a pure helium plasma is also included to demonstrate the strong  $Z$  dependence of these interactions.

### II. PERTURBATION-EXPANSION THEORY FOR COULOMB INTERACTION

The most rigorous theoretical method used in the study of the fully ionized gas interacting via the Coulomb potential is the perturbation expansion

of the many-body partition function and the concurrent use of Feynman diagram techniques. The divergence problems of the quantum-mechanical Coulomb gas have been illustrated by DeWitt<sup>7</sup> using a simple perturbation expansion of the first three terms. It is readily shown that the first-order perturbation term is canceled by the electroneutrality condition.

The second-order term of the simple perturbation expansion gives a linear divergence due to the long-range nature of the Coulomb interaction. This difficulty is resolved in the perturbation expansion of the partition function by summing the ring diagrams which are the most divergent pieces of the simple perturbation expansion. The resultant ring-diagram sum is finite, since the Coulomb potential is replaced by the dynamic screened potential. The ring sum and the appearance of the screened potential are equivalent to the random-phase approximation of Bohm and Pines.<sup>8</sup> The screened potential introduces a generalization of the Debye screening length and cuts off the linear divergence. The finite temperature quantum form of the ring sum due to Montroll and Ward<sup>2</sup> gives the Debye-Hückel (DH) result in the high-temperature or classical limit, and quantum corrections arising from the uncertainty principle. At zero temperature and high density, the ring sum gives the Gell-Mann-Brueckner correlation energy of the electron gas. For intermediate temperatures, it does not seem possible to evaluate the ring sum analytically; numerical evaluation is in progress.

The third-order term of the simple perturbation expansion produces a double logarithmic divergence: a long-range divergence as in the second-order term and a short-range divergence arising from the singularity at the origin. The quantum-perturbation method replaces the third-order term by a sum of higher-order terms, described by the Feynman ladder diagrams. In this term, two steps are required to remove the divergences. First, Coulomb-interaction chains are summed, producing a screened interaction between particle pairs, thus introducing the screening length and removing the long-range divergence. Second, the resulting ladder interactions with the screened potential are summed over all orders from three upward. For the classical gas this produces a cutoff, the average distance of closest approach  $\beta e^2 \langle Z^2 \rangle$ , which removes the short-range divergence. In the much more complex term for a two-particle quantum gas, the three-rung ladder term, the short-range cutoff in the quantum term is the de Broglie wavelength  $\lambda$  arising from the uncertainty principle.

In addition to the direct interactions, when a real multicomponent gas obeying Fermi-Dirac (FD) statistics is considered, a second series of

terms must appear in the perturbation expansion. These exchange-interaction terms arise from symmetry considerations, the operation of the exclusion principle. In general, for much of density and temperature space, the contribution of the exchange interactions is small compared to the direct terms, although they become dominant in the limit of low temperature or high density. The exchange terms have been evaluated to varying degrees of completeness for first-, second-, and third-order in the expansion.

In Secs. III-VI, these contributions to the free energy of a multicomponent, partially degenerate, strongly ionized gas will be studied individually by the free-energy minimization method. Since the present model is rigorous only in the high-temperature limit, we shall concentrate the analysis on a hydrogen plasma in this high-temperature region, whose limits as prescribed by internal validity constraints of the theory are  $50 \lesssim T \lesssim 2000$  eV. To examine the behavior of the model in a nonrigorous but physically interesting region, we also study hydrogen in a  $5 \leq T \leq 50$ -eV low-temperature region. Finally, the application of the theory to a more strongly interacting system, ionized helium, is briefly investigated.

### III. RING-SUM TERM FOR PARTIALLY DEGENERATE MULTICOMPONENT SYSTEMS

The perturbation expansion for a multicomponent fully ionized gas has as its leading term the quantum-mechanical ring sum, a quantum generalization of the classical electrostatic (DH) model, including both the effects of quantum statistics and of wave mechanics. As derived by Montroll and Ward<sup>2</sup> and DeWitt,<sup>6</sup> the ring sum has the general form

$$\beta F_{\text{ring}} = \frac{1}{2} V \sum_{\nu=-\infty}^{\infty} \int_0^{\infty} \frac{4\pi k^2 dk}{h^3} \{ \chi(k, \nu) - \ln[1 + \chi(k, \nu)] \}, \quad (1)$$

where

$$\chi(k, \nu) = (4\pi\beta e^2 / Nk^2) \sum_i Z_i^2 N_i \mathcal{L}(x_i^2, 2\pi i\nu) \quad (2)$$

and

$$x_i = \lambda_i k,$$

where  $\mathcal{L}(x_i^2, 2\pi i\nu)$  is the pair propagator.

This general form is analytically intractable and currently is being evaluated numerically. However, by suitable simplifications, it can be reduced to an approximate analytic form which is valid for multicomponent mixtures of charged particles, which obey either Maxwell-Boltzmann (MB) statistics or weakly degenerate FD statistics.

This approximate form for the multicomponent partially degenerate point-charge plasma is

$$\beta F_{\text{ring}} = - \sum_i N_i \frac{1}{3} \Lambda_F, \quad (3)$$

and

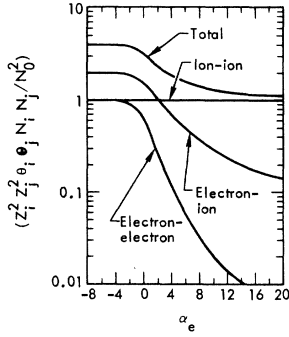


FIG. 1. Degeneracy effects for electron-electron, electron-ion, and ion-ion pair interactions.

$$\Lambda_F = 2\pi^{1/2} e^3 \beta^{3/2} (N/V)^{1/2} (\sum Z_i^2 N_i \theta_i / \sum N_i)^{3/2}, \quad (4)$$

where

$$\theta_i \equiv \frac{\mathcal{J}_{-1/2}(\alpha_i)}{\mathcal{J}_{+1/2}(\alpha_i)}, \quad \mathcal{J}_n(\alpha_i) = \frac{1}{\Gamma(n+1)} \int_0^\infty \frac{x^n dx}{e^{x-\alpha_i} + 1}. \quad (5)$$

In the classical limit, for weak interactions, this form reduces to the DH equation. This classical asymptotic form is a reasonably accurate calculation of Coulombic effects for  $\alpha \lesssim -4$ ,  $\Lambda \lesssim 0.3$ .

The plasma parameter, a dimensionless quantity representing the expansion parameter for the perturbation theory, is also directly related to the generalized screening length:

$$\Lambda_F = \frac{1}{4\pi n \lambda_F^3}, \quad (6)$$

$$\lambda_F = (4\pi \beta e^2 \sum Z_i^2 N_i \theta_i / V)^{-1/2}.$$

The region of density-temperature space where Eq. (3) can be expected to provide an accurate description of the Coulomb interactions is given by the restrictions  $\Lambda_F \lesssim 0.5$ ,  $\alpha_e \lesssim +2$ .

The first restriction relates to the importance of higher-order terms in the perturbation expansion; the second relates to the point where the quantum statistical approximations are no longer adequate. It is instructive to rewrite  $\Lambda_F$  in a form which more explicitly demonstrates both the pair nature of the perturbation and the effects of the quantum statistics on the interaction:

$$\Lambda_F = \lambda_F / 4\pi n \lambda_F^4 = \lambda_F (4\pi \beta^2 e^4 N / V) \times \frac{[Z_e^4 N_e^2 \theta_e^2 + 2Z_e^2 N_e \theta_e \sum Z_i^2 N_i \theta_i + \sum \sum Z_i^2 Z_j^2 N_i N_j \theta_i \theta_j]}{(\sum N_i)^2}, \quad (7)$$

where the three terms in square brackets represent, respectively, the electron-electron, the electron-ion, and the ion-ion Coulomb interactions. In the classical limit, the  $\theta_i$ 's approach 1, and the full expression is identical to the DH theory for point charges. In the direction of increasing degeneracy,  $\theta_e$  changes monotonically from its classical value of 1 towards 0.

The relative contributions to the total ring-sum

free energy are illustrated in Fig. 1. The electron-electron term contributes one-fourth of the total in the classical limit, decreasing as  $\theta_e^2$  to 0.114 at  $\alpha_e = +2$ .

The electron-ion term contributes one-half of the total ring sum in the classical limit, and decreases as  $\theta_e$  to 0.444 by  $\alpha_e = +2$ . The strength of the ion-ion term is unaffected by degeneracy until very high densities are reached. If the partial degeneracy approximation is carried out to higher values of  $\alpha_e$ , it shows the electron-electron term decreasing to a negligible value at  $\alpha_e = +20$  and the electron-ion term dropping to 0.13 of the total. The degeneracy factors for the ions ( $\theta_i, \theta_j$ ) are unity for all regions studied in this paper, so that even in the limit of high electron density the ion-ion term retains its low-density form.

The quantum-mechanical ring sum has additional analytical features which extend its region of applicability. In addition to the inclusion of effects of quantum statistics, DeWitt has evaluated the ring sum at finite temperature.<sup>9</sup> In the high-temperature limit where all particles obey MB statistics, the quantum ring sum reduces to a classical ring sum times an asymptotic expansion in powers of  $\gamma$ , the quantum diffraction parameter. This function arises solely from the operation of the uncertainty principle, and thus embodies the wave-mechanical effects present in the high-temperature plasma. The expansion is in powers of a wave-mechanical diffraction parameter defined by

$$\gamma_i \equiv \lambda_i / \lambda_F, \quad \lambda_i = \hbar / (2m_i kT)^{1/2},$$

$$\gamma_{ei} = \lambda_{ei} / \lambda_F, \quad \lambda_{ei} = \hbar / (2\mu_{ei} kT)^{1/2}, \quad (8)$$

$$\mu_{ei} = m_e m_i / (m_e + m_i).$$

It should be noted here that there are two forms for the  $\gamma$  parameters, a single-particle form  $\gamma_i$  containing the single-particle mass, and a pair form  $\gamma_{ei}$ , containing the reduced mass of the interacting pair. The various  $\gamma$ 's are ordered as

$$[\gamma_{ee} \sim (2/m_e)] > \left[ \left( \gamma_{ei} \sim \frac{1+m_e/m_i}{m_e} \right)^{1/2} \right]$$

$$\approx [\gamma_e \sim (1/m_e)^{1/2}] > [\gamma_{ii} \sim (2/m_i)^{1/2}]$$

$$> [\gamma_i \sim (1/m_i)^{1/2}]. \quad (9)$$

The application of this wave-mechanical correction is restricted to regions of density-temperature space where  $\alpha_e \leq -4$  and  $\Lambda < \gamma_i$ . This latter restriction is equivalent to  $\beta e^2 \langle Z^2 \rangle < \lambda_i$ .

The wave-mechanical correction is given by the term in curly brackets:

$$\beta F_{\text{ring}} = -\sum N_i \frac{1}{3} \Lambda_F \{P(\gamma)\},$$

$$P(\gamma) = 1 - \frac{1}{16} 3\pi^{1/2}$$

$$\begin{aligned} & \times \left( \frac{Z_e^4 N_e^2 \gamma_{ee} + 2Z_e^2 Z_i^2 N_e N_i \gamma_{ei} + Z_i^2 Z_j^2 N_i N_j \gamma_{ij}}{N^2 \langle Z^2 \rangle^2} \right) + \frac{1}{4} \gamma_e^2 \\ & \times \left( \frac{Z_e^4 N_e^2 + Z_e^2 Z_i^2 N_e N_i (1 + m_e/m_i) + Z_i^4 N_i^2 (m_e/m_i)}{N^2 \langle Z^2 \rangle^2} \right). \end{aligned} \quad (10)$$

An additional restriction on the use of this form is that  $\gamma^2 < \gamma_c^2$ , where  $\gamma_c$  represents that value of  $\gamma$  where the full asymptotic series begins to diverge. For the one-component gas, this value is found analytically to be  $\gamma_c^2 = 2.042$ . For multicomponent gases, the value of  $\gamma$  where the two term series given above starts to diverge depends on the charge of the gas ions.

The wave-mechanical correction is illustrated in Fig. 2 for fully ionized gases with ions of charge  $Z = 1, 2$ , and 6. For hydrogen, the minimum value attained is 0.83 at  $\gamma$  of 1.14. As  $Z$  increases, the minimum value of  $P(\gamma)$  and the value of  $\gamma$  at this point both increase. It is clear that this asymptotic form is limited to the region  $0 < \gamma < 1.1$  for hydrogen.

Both the statistical and wave-mechanical effects extend the range of applicability of the ring-sum term, but there are large regions of density-temperature space where both these limiting forms are insufficient. Specifically, in the high-density limit, the ion-ion term causes an eventual divergence of the ring sum, a failure which is accompanied by the appearance of negative pressures and energies. This short-range divergence can be removed only by a rigorous theory which includes all terms in the  $n$ th-order perturbation expansion, or as many terms as are necessary to remove the singularity. Since this high-order quantum-mechanical sum evaluation is not feasible at present, various empirical models have been proposed to represent this correct approach.

In the theory of a classical electrostatic system of extended (nonpoint) charges, there is a straightforward approach used to incorporate the finite size of the charged particles. This approach has the effect of removing the divergence by introduction of a short-range cutoff length. The procedure results in a function  $\tau(x)$  which is called a finite-ion-size correction. For a dilute plasma containing ions with electronic orbitals, this model can be directly applied: For the short-range limit of the interaction integral, one uses the effective radius of the outer electron orbital. These radii, for such systems as  $H^+$ ,  $He^+$ ,  $Li^{+2}$ , can be approximated from experimental data, or from self-consistent field calculations of the free-atom charge-density distributions.

For fully ionized nuclei, a short-range cutoff of the Coulomb interaction must be chosen from one of the available characteristic lengths of the system. An obvious candidate is the average dis-

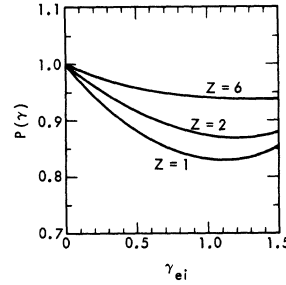


FIG. 2. Wave-mechanical corrections for fully ionized two-component gases of nuclear charge 1, 2, and 6.

tance of closest approach of two nuclei  $\beta e^2 Z_i Z_j$ , the classical turning point, and a reasonable estimate for the short-range limit of a repulsive interaction. This distance is modified by the fact that the nuclei can be considered to be interacting via a screened Coulomb potential, whose associated generalized screening length contains the effects of quantum statistics on the electron interactions. Taking this into consideration, a screened distance of closest approach can be defined as

$$l_s = \beta e^2 Z_i Z_j e^{-1s/\lambda_F}, \quad (11)$$

which reduces to the unscreened value  $l_c$  when  $l_s \ll \lambda_F$ , and which is significantly smaller than  $l_c$  when  $l_s \gtrsim \lambda_F$ . The functional form of the finite-ion-size correction is given by

$$\tau(x) = 3 \left[ \ln(1+x) - x + \frac{1}{2} x^2 \right] x^{-3}, \quad (12)$$

where

$$x = r_{\min}/\lambda_F,$$

and  $r_{\min}$  is the effective radius of the outer orbital for extended species, and is  $l_s$  for the bare nuclei. This modification when combined with the foregoing definition of the ring term gives a total configurational Coulombic free energy of the following form:

$$\begin{aligned} \beta(F_4)_{\text{ring}} = & -\sum N_i \frac{1}{3} \lambda_F (4\pi\beta^2 e^4 \sum N_i/V) (Z_e^4 N_e^2 \theta_e^2 \\ & + 2Z_e^2 N_e \theta_e \sum Z_i^2 N_i \theta_i \tau(x_i) \\ & + \sum \sum Z_i^2 Z_j^2 N_i N_j \theta_i \theta_j \tau(x_{ij})) / (\sum N_i)^2. \end{aligned} \quad (13)$$

The finite-ion-size correction in the electron-ion term is never significant for the hydrogen plasma considered here. This is true because extended charged species ( $H_2^+$ ,  $H^+$ ) are everywhere trace constituents, while repulsive electron-ion interactions are only operative for the  $H^+$  ion. The finite-ion-size correction can become quite large for the ion-ion interaction, specifically for the  $H^+-H^+$  contribution. However, in the region of density-temperature space where the full perturbation-expansion model presented here is strictly valid, this correction never reduces the ion-ion term by more than 10%.

#### IV. FIRST-, SECOND-, AND THIRD-ORDER EXCHANGE INTERACTIONS FOR ELECTRONS

The total partition function for a real gas should include terms representing the exchange interactions between free particles of equal spin. The simplest exchange interaction, treated in first-order perturbation theory, gives for the free energy of the gas<sup>8</sup>

$$\beta(F_4)_{1x} = -\frac{N_i \gamma_i^2}{2(2s_i + 1)} \iint \frac{d\vec{y}_1 d\vec{y}_2}{\pi^3 \xi_i^2} \frac{f^-(\vec{y}_1) f^-(\vec{y}_2)}{|\vec{y}_1 - \vec{y}_2|^2}. \quad (14)$$

This can be rewritten in terms of the Fermi functions for a fermion gas as<sup>10</sup>

$$\beta(F_4)_{1x} = -\frac{N_i \gamma_i^2}{(2s_i + 1) \xi_i^2} \int_{-\infty}^{\alpha} d\alpha' \mathcal{G}_{-1/2}^2(\alpha'), \quad (15)$$

where

$$\gamma_i = (\kappa_i / \lambda_D) (Z_i^2 N_i / \sum Z_i^2 N_i)^{1/2}, \quad (16)$$

$$\lambda_D = (4\pi\beta e^2 \sum Z_i^2 N_i / V)^{-1/2},$$

which becomes, for electrons,

$$\beta(F_4)_{1xe} = -N_e \frac{1}{2} \gamma_e^2 \frac{N_e}{\sum Z_i^2 N_i} \frac{\int_{-\infty}^{\alpha_e} d\alpha' \mathcal{G}_{-1/2}^2(\alpha')}{\mathcal{G}_{1/2}^2(\alpha_e)}. \quad (17)$$

This general form of the first-order exchange interaction for electrons can be simplified in two limiting cases. First, for the classical electron gas,

$$\lim_{\alpha_e \ll -1} \left( \int_{-\infty}^{\alpha_e} d\alpha' \mathcal{G}_{-1/2}^2(\alpha') / \mathcal{G}_{1/2}^2(\alpha_e) \right) = \frac{1}{2}. \quad (18)$$

Thus, we have

$$\beta(F_4)_{1xe} = -N_e \frac{1}{4} \gamma_e^2 (N_e / \sum Z_i^2 N_i). \quad (19)$$

In the region of the completely degenerate electron gas, Wasserman, Buckholtz, and DeWitt<sup>11</sup> find that

$$\lim_{\alpha \gg +1} 2 \int_{-\infty}^{\alpha} d\alpha' \mathcal{G}_{-1/2}^2(\alpha') = (4/\pi) \alpha^2 - \frac{2}{3} \pi \ln \alpha + C_3, \quad (20)$$

$$C_3 = -3 + 3 \ln 2 + \gamma + (12/\pi^2) (-0.10131658),$$

so that

$$\lim_{\alpha \gg +1} \beta(F_4)_{1xe} = -N_e \frac{1}{2} \gamma_e^2 \frac{N_e}{\sum Z_i^2 N_i} \times \frac{1}{2} \frac{(4/\pi) \alpha^2 - \frac{2}{3} \pi \ln \alpha + C_3}{[(4/3\sqrt{\pi}) \alpha^{3/2}]^2}. \quad (21)$$

The functional form of the exchange term is shown in Fig. 3. The classical asymptote provides a good approximation for values  $-\infty \leq \alpha \leq -1.5$ , while the complete degeneracy asymptote is reasonably accurate over the range  $+\infty \leq \alpha \leq +5$ .

Inclusion of the general first-order exchange term, or either of the asymptotic forms where valid, treats the exchange partition function ex-

actly to first order. Higher-order perturbation terms are available; however, the labor required to calculate them accurately is extensive. The second-order exchange term is known analytically for that physical region where MB statistics apply to the electrons<sup>7</sup>:

$$\beta(F_4)_{2xe} = -N_e \frac{\pi^{3/2}}{2^{7/2}} (\ln 2) \frac{\Lambda_F \gamma_e}{2s_e + 1} \left( \frac{Z_e^2 N_e}{Z_i^2 N_i} \right)^{1/2}. \quad (22)$$

The second-order exchange term in this limit is evidently of the same form as the wave-mechanical corrected ring term. In general, contributions to the ring term of order  $\Lambda \gamma^n$  should be accompanied by the corresponding exchange term of the same order. The restrictions on the use of this form of the second-order exchange are that  $\alpha_e \leq -4$ .

The third-order exchange term for electron-electron interactions is also too difficult to evaluate for arbitrary degeneracy at present. However, there is an analytic evaluation which is valid for the region of MB statistics, derived by Hoffman and Ebeling<sup>12</sup>:

$$\beta(F_4)_{3xe} = -N_e (\Lambda_0^3 / 12 \Lambda_F) [N_e^2 / (\sum N_i)^2] D_x, \quad (23)$$

where  $D_x = \frac{1}{24} \pi^2$  and  $\Lambda_0 = \beta e^2 / \lambda_F$ .

#### V. THREE-RUNG LADDER TERM

A major advantage of the perturbation expansion is that it permits a systematic extension of the many-body plasma partition function to a quantum theory of higher-order terms. The expansion term beyond the ring-sum term in the quantum cluster expansion is the three-rung ladder term  $S_2$ . It describes direct interactions involving three and more scatterings of two particles via the dynamic screened Coulomb potential.

The exact quantum-mechanical form for  $S_2$  is a complex multidimensional integral which is far more difficult to evaluate than the ring integral of Eq. (1). The exact result for this integral in the high-temperature limit has been solved analytically by Hoffman and Ebeling.<sup>12</sup> The high-temperature limit is defined here as the region of classical statistics, where the plasma lengths obey the following order:

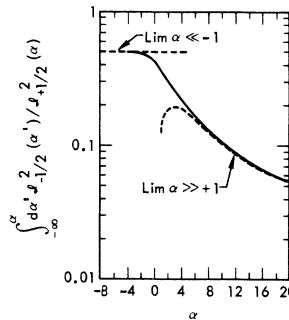


FIG. 3. The exchange integral as a function of degeneracy compared to Maxwellian and completely degenerate asymptotic limits.

$$\bar{\lambda}_{ii} < \beta e^2 \langle Z^2 \rangle < \bar{\lambda}_{ei}, \quad \bar{\lambda}_{ee} < \lambda_D, \quad (24)$$

which gives an ordering of the dimensionless parameters of

$$\gamma_{ii} < \Lambda < \gamma_{ei}, \quad \gamma_{ee} < 1. \quad (25)$$

This set of restrictions, when applied to a fully ionized hydrogen gas, corresponds to a temperature range  $50 \lesssim T \lesssim 2000$  eV.

The limiting form of the three-rung ladder is then

$$\begin{aligned} \beta(F_4)_{3L} &= - \sum N_i S_2, \\ S_2 &= \frac{1}{12} \Lambda^2 \{ Z_e^6 N_e^2 (\ln \gamma_{ee} + D_Q) + 2 Z_e^3 N_e \sum Z_i^3 N_i \\ &\quad \times (\ln \gamma_{ei} + D_Q) + \sum \sum Z_i^3 Z_j^3 N_i N_j \\ &\quad \times [\ln(Z_i Z_j \beta e^2 / \lambda_D) + D_c] \} / N^2 \langle Z^2 \rangle^2, \quad (26) \end{aligned}$$

where  $D_c = 0.41974$  and  $D_Q = 0.88722014$ . The first term describes the electron-electron interaction, the second, the electron-ion interaction, and the third, the ion-ion interaction. Much heavier than the electrons, the ions operate as purely classical particles everywhere in this region. However, the electron interactions exhibit wave-mechanical effects in the high-temperature region. Because of the  $Z^3$  dependence, the three terms in  $F_2$  do not have the same sign and combine in a destructive manner rather than in a constructive manner, as did the individual components of the ring sum. Thus, in the high-temperature region, the total three-rung ladder term tends to be always smaller than the individual terms which combine to form it.

Since the exact asymptotic form is valid only in the region where the three-rung ladder makes small corrections to the ring-sum term, an approximate form of the quantum-mechanical ladder term has been developed. This integral expression incorporates both quantum-statistical effects and wave-mechanical effects into the higher-order perturbation term, and hence should apply over a wider range of physical space than the exact asymptotic form. It does recover this exact form in the high-temperature limit. The partially degenerate multi-component integral equation for the approximate three-rung ladder is

$$\begin{aligned} \beta(F_4)_{3L} &= - \sum N_i S_2(\Lambda, \gamma), \\ S_2 &= (1/2\Lambda_F) \{ (N_e^2/N^2) \int_{\alpha_1 \gamma_{ee}}^{\infty} S'_2(\Lambda_{ee}) + (2N_e/N^2) \\ &\quad \times \sum N_i \int_{\alpha_1 \gamma_{ei}}^{\infty} S'_2(\Lambda_{ei}) \\ &\quad + \sum \sum (N_i N_j / N^2) \int_{\alpha_3 \gamma_{ij}}^{\infty} S'_2(\Lambda_{ij}) \}, \quad (27) \end{aligned}$$

where

$$\Lambda_{ki} = Z_k Z_i \beta e^2 / \lambda_F \quad (28)$$

and

$$\begin{aligned} S'_2(\Lambda_{ki}) &= x^2 dx \{ \exp(-\Lambda_{ki} e^{-x}/x) - 1 + \Lambda_{ki} (e^{-x}/x) \\ &\quad - \frac{1}{2} [\Lambda_{ki} (e^{-x}/x)]^2 \}. \quad (29) \end{aligned}$$

The value of  $a_1$  (0.454575) is determined by requiring the integral expression for  $S_2$  to recover the exact form in the limit of high temperature.

The integral

$$\int_a^{\infty} x^2 (e^{-a} - 1 + q - \frac{1}{2} q^2) dx,$$

where  $q = (\Lambda/x) e^{-x}$  cannot be evaluated analytically and is somewhat difficult to do numerically.

The simplest procedure seems to be to divide the interval of integration into three separate sub-intervals. In the interval where  $x \geq c$ , and  $c$  is sufficiently large so that  $(|\Lambda|/c) e^{-c} \ll 1$ , we can expand the  $e^{-a}$  in the integrand and the integral becomes

$$\int_c^{\infty} x^2 \sum_{n=3}^{\infty} \frac{(-1)^n \Lambda^n e^{-nx}}{n! x^n} dx. \quad (30)$$

The individual terms in this series are difficult to integrate numerically if  $a \ll 1$ , but fortunately by use of the definition

$$E_m(Z) \equiv \int_1^{\infty} (e^{-zt}/t^m) dt, \quad (31)$$

we can rewrite the series as

$$\sum_{m=3}^{\infty} \frac{(-\Lambda)^m}{c^{m-3} m!} E_{m-2}(mc); \quad (32)$$

and by using the recursion relation

$$E_m(Z) = \frac{e^{-Z}}{m-1} - \frac{Z}{m-1} E_{m-1}(Z), \quad m > 1 \quad (33)$$

the integral from  $a$  to  $\infty$  becomes

$$\begin{aligned} & - \frac{1}{6} \Lambda E_1(3c) + (\Lambda^4/24c) [e^{-4c} - 4c E_1(4c)] \\ & - (\Lambda^5/240c^2) [(1-5c)e^{-5c} + 25c^2 E_1(5c)] + \dots \quad (34) \end{aligned}$$

The exponential integral  $E_1(Z)$  can be evaluated comparatively easily, and the above series converges quite rapidly when  $c$  is large enough that  $q \lesssim 0.2$ .

In the case  $\Lambda > 0$ , there may exist an interval  $a < x < b$  such that  $(\Lambda/b) e^{-b} \gg 1$ . In this interval  $e^{-a}$  may be neglected in the integrand, and the remaining part may be integrated analytically giving

$$\begin{aligned} \int_a^b x^2 (-1 + q - \frac{1}{2} q^2) dx &= \frac{1}{3}(a^3 - b^3) + \Lambda(ae^{-a} - be^{-b}) \\ &+ \Lambda(e^{-a} - e^{-b}) + \frac{1}{4} \Lambda^2(e^{-2b} - e^{-2a}). \quad (35) \end{aligned}$$

In the case  $\Lambda > 0$  for  $b < x < c$ , the integrand is quite well behaved, and it is no problem to integrate numerically.

The one remaining case is for  $\Lambda < 0$  and  $|q|$  not small. The integral diverges in the limit  $a \rightarrow 0$ , and is quite difficult to evaluate even numerically for small values of  $a$ , because of the  $x^{-1}$  term in

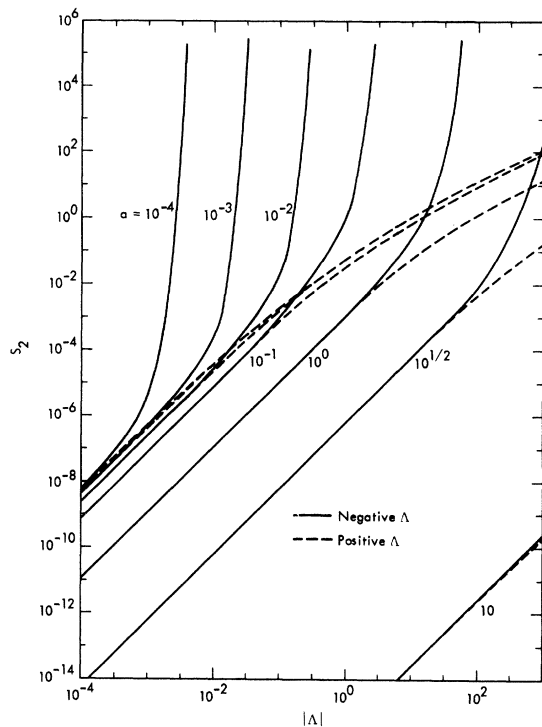


FIG. 4. The general form of the three-rung ladder terms  $S_2(\Lambda, a)$  as a function of the interaction parameter  $\Lambda$ . The parameter  $a$  is the lower limit of the integral.

the exponential of the integrand. The numerical integration may be accomplished efficiently by means of QUAD 4, a general-purpose numerical integration routine written by one of the authors (DJH) in the FORTRAN language.

Combining the above procedures, the integral may be evaluated quite rapidly and accurately on a computer for all values of  $\Lambda$  and all  $a > 0$  except those ( $\Lambda < 0$  and  $a \ll |\Lambda|$ ) where overflows occur in the machine.

The results of the complete numerical evaluation of  $S_2(\Lambda, a)$  are given in Figs. 4 and 5. In Fig. 4, the values of  $S_2$  are plotted for  $-10^3 \leq \Lambda \leq +10^3$  and  $10^{-4} \leq a \leq 10^1$ . The equality of  $S_2$  for positive and negative  $\Lambda$  is seen where  $\Lambda/a < 1$ . For positive  $\Lambda$ , the limiting asymptote ( $a=0, \Lambda \gg 1$ ) is represented by the  $a=10^{-4}$  curve. At sufficiently large positive  $\Lambda$ , and  $|q|$  not small, the integral becomes an extremely sensitive function of  $\Lambda$ , as can be seen from the negative  $\Lambda$  curves of Fig. 4. This region corresponds physically to the case of electron-ion interactions, and hence is an important region in a real gas.

If we restrict the region of  $(\Lambda, a)$  space considered to that where the present theoretical considerations are significant and valid, the illustration in Fig. 5 covers all cases of interest. In most ionized gas regions,  $\Lambda < 10^{-2}$  presents negligible corrections to

the ideal gas while  $\Lambda > 10$  requires a more extensive theoretical approach. Similarly, values of  $S_2$  for  $a < 10^{-3}$  are reasonably approximated by  $S_2$  for  $a = 10^{-3}$ , while  $S_2$  for  $a > 10$  gives negligibly small contributions. Hence, for most gas problems, the range presented in Fig. 5 is adequate to describe electron-electron, ion-ion (positive  $\Lambda$ ), and electron-ion (negative  $\Lambda$ ) interactions.

The total Coulomb configurational free energy combining all the free-energy terms is then given by

$$F_4 = (F_4)_{\text{ring}} + (F_4)_{1\text{xe}} + (F_4)_{3L} + (F_4)_{2\text{xe}} + (F_4)_{3\text{xe}},$$

where the ring term is given by Eq. (13), first-order exchange by Eq. (17), the three-rung ladder by Eq. (27), second-order exchange by Eq. (22), and third-order exchange by Eq. (23).

## VI. THERMODYNAMIC-EQUILIBRIUM EFFECTS

The foregoing theoretical model has been included as the Coulomb configurational free energy of a multicomponent gas. The total free energy is, except for the Coulomb term, identical to the final model of Paper I. The ideal gas is modified by inclusion of a confined atom model of the bound-state perturbation and a hard-sphere mixture model for the excluded volume configurational term. Minor interaction terms include a van der Waals's type, long-range molecular attraction, and the photon gas free energy. The free-energy minimization method is used to calculate the thermodynamic properties

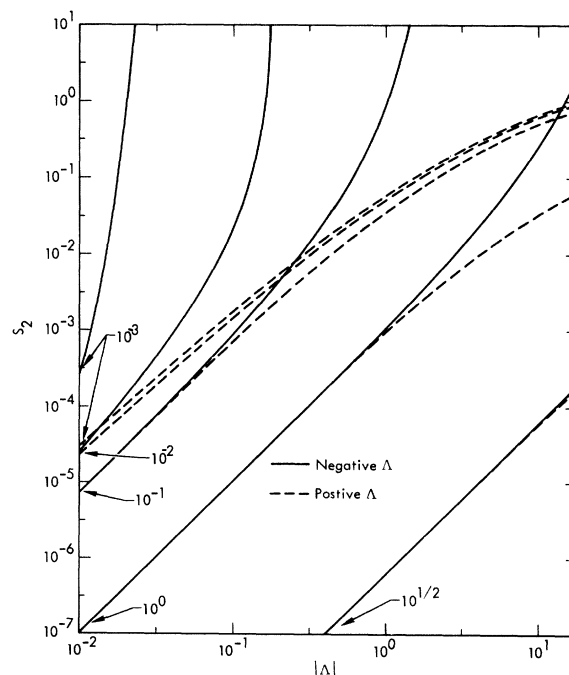


FIG. 5. The functional form of the three-rung term for the range of physical interest.

of hydrogen and helium gas mixtures.

The hydrogen system studied consists of a six-component mixture ( $H_2, H_2^+, H^-, H^+, e^-$ ) with an initial composition of one mole of  $H_2$ . The primary temperature region examined is  $50 \leq T \leq 2000$  eV, where  $H, H^+$ , and  $e^-$  are the only significant constituents. This high-temperature regime is chosen for several reasons. First, it minimizes the importance of the other nonideal terms (bound-state perturbation and excluded volume term) and allows the Coulomb interactions to dominate. Second, it restricts  $\alpha_e$ , the electron degeneracy, to near-classical values and restricts  $\Lambda_F$  to small or moderate values. These restrictions are necessary for the present form of the ring term to be valid, and for the second-order Coulomb term to be smaller than the ring term. Third, this choice causes  $\Lambda_F/\gamma_{eH} \lesssim 1$ , which is the validity requirement for the asymptotic form of  $S_2$  and for the wave-mechanical correction to the ring term.

In the previous study, the inclusion of a simpler model of the Coulomb interaction was found to increase ionization and to decrease the total pressure over a wide density-temperature range. A similar result is obtained here, as demonstrated by the results for hydrogen given in Fig. 6. In the figure, the total mole number (one initial mole of  $H_2$  ionizes to four moles of plasma) exhibits strong ionization at all volumes for all six isotherms. The primary mechanism for nonideal ionization here is still the bound-state perturbation, and the Coulomb effects contribute a maximum ionization enhancement of 0.3%.

Since the Coulomb configurational term makes very minor changes in the ionization equilibrium in this high-temperature region, a lower-temperature regime was calculated,  $5 \leq T \leq 50$  eV. Here, the contributions of the various Coulomb perturbation-expansion terms are more readily separable, as shown in Table I. The ionization for the full

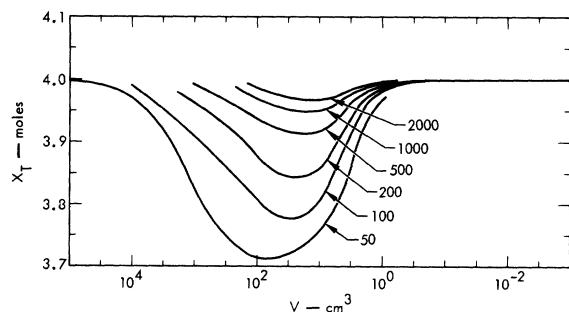


FIG. 6. Ionization equilibrium of hydrogen for temperatures of 50–2000 eV. The fully ionized gas consists of 4.0 moles of ions and electrons. At the ionization minimum on the 50-eV isotherm, the atomic hydrogen is 86% ionized.

TABLE I. Ionization equilibrium of hydrogen for various Coulomb-interaction free-energy models.

$V$ ( $cm^3$ )	$T$ (eV)			
	5	10	20	50
$10^6$	3.9984 <sup>a</sup>	3.9964	3.9986	...
	3.9887 <sup>b</sup>	3.9965	3.9986	...
	3.9887 <sup>c</sup>	3.9965	3.9986	...
	3.9888 <sup>d</sup>	3.9965	3.9986	...
$10^5$	3.8955	3.9654	3.9879	3.9968
	3.9027	3.9664	3.9879	3.9968
	3.9027	3.9664	3.9879	3.9968
	3.9035	3.9664	3.9879	3.9968
$10^4$	3.4888	3.7397	3.8925	3.9710
	3.5450	3.7559	3.8956	3.9712
	3.5453	3.7559	3.8957	3.9712
	3.5566	3.7566	3.8957	3.9712
$10^3$	3.1614	3.5042	3.6683	3.8201
	3.3477	3.5568	3.6835	3.8229
	3.3514	3.5573	3.6837	3.8230
	3.4102	3.5623	3.6840	3.8229
$10^2$	2.6848	3.2670	3.5082	3.7026
	3.2233	3.4448	3.5645	3.7145
	3.2624	3.4521	3.5661	3.7146
	3.3410	3.4660	3.5678	3.7147
50	2.6116	3.2043	3.4846	...
	3.2815	3.4618	3.5602	...
	3.3511	3.4763	3.5632	...
	3.3663	3.4981	3.5654	...
20	2.7950	3.2232	3.4988	...
	3.4250	3.5394	3.6029	...
	3.5322	3.5681	3.6097	...
	3.4978	3.5674	3.6114	...
10	3.1464	3.4084	3.5888	3.7415
	3.5879	3.6527	3.6845	3.7515
	3.7049	3.6904	3.6937	3.7516
	3.6249	3.6773	3.6935	3.7517
5	3.4825	3.6237	3.7215	...
	3.7125	3.7731	3.7946	...
	3.8085	3.8103	3.8051	...
	3.7401	3.7927	3.8028	...
2	3.7674	3.8349	3.8804	...
	3.8541	3.8972	3.9169	...
	3.9101	3.9237	3.9258	...
	3.8654	3.9095	3.9229	...

<sup>a</sup>No Coulomb interaction included.

<sup>b</sup>Ring-sum term included.

<sup>c</sup>Ring-sum plus first- and second-order-exchange terms included.

<sup>d</sup>Full Coulomb-interaction model.

nonideal models is compared for (a) no Coulomb interaction, (b) ring term only, (c) ring plus first- and second-order exchange, (d) ring plus first-, second-, and third-order exchange plus the three-rung ladder. At the lower temperatures, the ionization enhancement of the ring term is clearly evident, reaching a maximum of 26% at 5 eV and

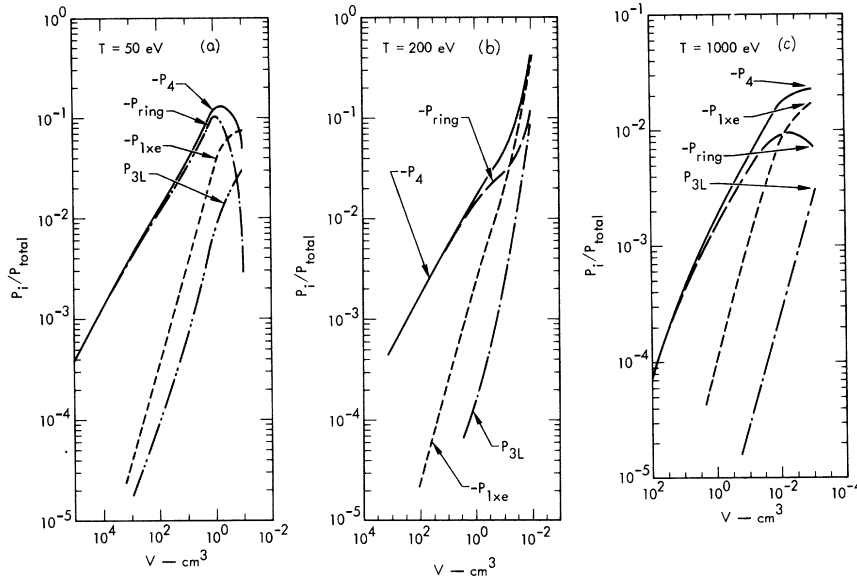


FIG. 7. (a) The ratios of the total Coulomb, ring, first-order-exchange, and three-rung-ladder pressure contributions to the total pressure at 50 eV. The total Coulomb, ring, and first-order-exchange pressures are negative. (b) Coulomb pressure contributions at 200 eV. (c) Coulomb pressure contributions at 1000 eV.

50 cm<sup>3</sup>. The addition of the first-order exchange term increases the ionization even further, although the effect is smaller: a maximum of 4% at 5 eV and 20 cm<sup>3</sup>. The addition of the three-rung ladder shows an interesting reversal. At low densities, where  $F_{4(3L)}$  is a negative function of  $\Lambda$ , the three-rung ladder term enhances ionization. This effect is smaller than the ring-term effect but larger than the exchange effects and occurs for  $V \lesssim 50$  cm<sup>3</sup>. As  $\Lambda_F$  increases,  $F_{4(3L)}$  changes sign, and the ladder term begins to inhibit ionization. This effect is still small even at 5 eV, and now is dominated by both ring and exchange contributions. By 50 eV in hydrogen, all these terms produce relatively small effects in the equilibrium composition.

A much stronger effect is seen when the equations of state are examined. The pressure corrections contributed by the Coulomb interaction are generally the largest nonideal corrections throughout the high-temperature region. The total Coulomb pressure effect and the individual contributions of the separate terms in  $F_4$  are illustrated in Fig. 7, where they are given as fractions of the total pressure. The  $P_4$ ,  $P_{ring}$ , and  $P_{1xe}$  are negative pressures, while  $P_{3L}$  is a positive pressure. The low-density functional dependence of the three terms are  $(P_4)_{ring}/P_{total} \sim \Lambda \sim V^{-1/2}$ ;  $P_{1xe}/P_{total} \sim \gamma_e^2 \sim V^{-1}$ ;  $P_{3L}/P_{total} \sim \Lambda^2 \ln \Lambda \sim V^{-1.5}$ . These approximate forms quite closely match the numerical results at low density. At higher density, the ring-term pressure departs from this limiting behavior, because of recombination and pressure ionization, to electron degeneracy and finally to the operation of a strong short-range cutoff factor  $\tau(x)$ . Electron degeneracy also begins to cause  $P_{1xe}$  to decrease from its low-density  $V^{-1}$  dependence. The major

conclusion apparent from these results is that the ring term is, as expected, the largest contributor at low density. The sharp turnaround observed at 50 and 1000 eV is due to the onset of electron degeneracy and the short-range cutoff. This latter effect is obviously crucial, since  $P_4$  is a moderate fraction of  $P_{total}$ , and if  $P_{ring}$  were to continue to rise at its low-density rate, the negative Coulomb correction would soon exceed the positive pressure. This indicates the importance of a complete evaluation of the exact quantum-mechanical ring sum for an ion-electron system. This task is being carried out by numerical integration on a computer, and will allow replacement of the approximate form used here Eq. (13) by an exact theoretical result.

The second conclusion is that the exchange pressure is an important contributor, even at reasonably moderate values of the electron degeneracy. Exchange reaches 5% of the total pressure at values of  $\alpha_e$  ranging from 0 (at 50 eV) to +5 (1000 eV), the region of slight-to-moderate degeneracy. At all three temperatures in Fig. 7, exchange becomes the largest contributor to the Coulomb pressure at the end of the isotherm. Generally, exchange pressure is not included in high-temperature or low-density Coulomb models until the gas is nearly completely degenerate. This leads to an underestimate of the Coulomb correction for all equations of state.

The three-rung ladder term is the smallest contributor everywhere, as is expected for this low  $\Lambda$  region. However, this term does rise rapidly with increasing density, and at the end of the three isotherms, it is approaching the ring term, although by the time this occurs the exchange pres-

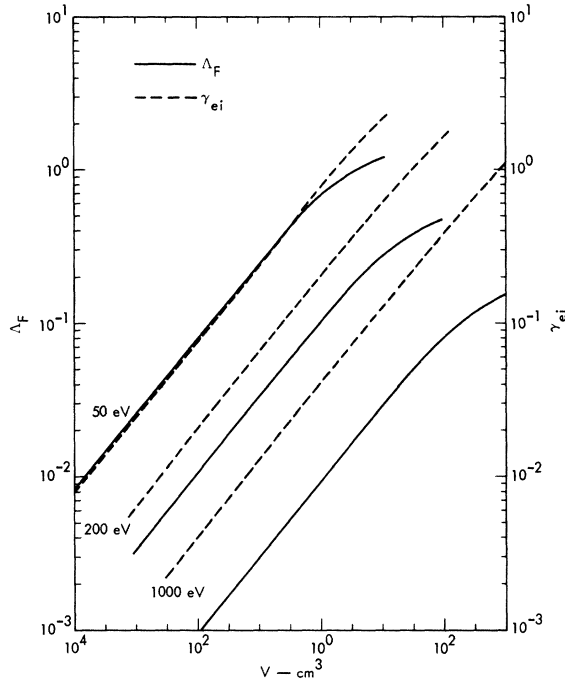


FIG. 8. The plasma interaction parameter  $\Lambda_F$ , and the quantum diffraction parameter  $\gamma_{ei}$  for ionized hydrogen in the range  $50 \leq T \leq 1000$  eV.

sure has become dominant. In general, the extension of the perturbation-expansion theory to include terms beyond the ring term (a process intended to reduce the divergence of the Coulomb partition function and to extend the range of positive accurate pressure calculations) has the effect of making the pressure more negative throughout the weak-to-moderate interaction region. In addition to the quantum-mechanical ring sum, a strong need is apparent for a correct calculation of the second-order exchange term for degenerate electrons, which acts to decrease the total exchange pressure. It should be noted here that in these calculations, the second- and third-order exchange terms were included only in the classical region, since the analytical forms of Eqs. (22) and (23) are valid only for MB statistics.

An examination of the dimensionless parameters characterizing the strongly ionized gas provides an estimate of the validity of the various terms. In Fig. 8,  $\Lambda_F$  and  $\gamma_{ei}$  are plotted for three isotherms of hydrogen. The lowest isotherm (50 eV) has  $\Lambda_F/\gamma_{ei} \sim 1$ , indicating that the wave-mechanical correction is marginally valid here, but should be accurate for  $T > 50$  eV. Also, the asymptotic  $S_2$  form should be accurate at the low-density end of the isotherm. At 200 and 1000 eV, the value of  $\Lambda_F/\gamma_{ei}$  drops to  $\sim \frac{1}{2}$  and  $\sim \frac{1}{4}$ . At the high-density end of all three isotherms, electron degeneracy and short-range cutoff effects cause a marked de-

crease in the volume dependence of  $\Lambda_F$ . The degeneracy effects are exhibited in Fig. 9, where  $\Lambda_F$  and  $\alpha_e$  are plotted for the full  $V, T$  range considered. The range of  $\Lambda_F$  is from  $10^{-3}$  (Coulomb corrections negligible) to 1 (three-rung ladder necessary), while  $\alpha_e$  ranges from  $-12$  (highly Maxwellian) to  $+4$  (moderately degenerate, exchange effects dominant).

A comparison of the analytically correct wave-mechanical correction  $P(\gamma)$  and the empirical finite-ion-size correction  $\tau(x)$  is given for hydrogen in Fig. 10. The wave-mechanical correction reaches minimum values in the range 0.82–0.86 for the temperature range 50–2000 eV, with the minimum occurring at  $\gamma_{ei}$  of about 1.15. For  $\gamma_{ei} > 1.15$  there is a sharp reversal as  $P(\gamma)$  becomes larger than unity, due to divergence of the two-term asymptotic series.

The finite-ion-size correction exhibits somewhat different behavior, as shown in the Fig. 10. There are several  $\tau(x_i)$  terms, corresponding to the various ion-ion pair interactions ( $H^-H^+$ ,  $H_2^-H_2^+$ ,  $H^+H^+$ ), but the only one which is operative in the strongly ionized gas is the short-range cutoff for  $H^+H^+$  interactions. When this factor is compared with the  $P(\gamma)$  behavior, it is clear that there is quite good qualitative agreement – the two factors have almost identical volume dependence over the complete range of  $V$  studied. Their quantitative agreement is also reasonably good: At 200 eV they differ by less than one-half of 1%. For  $T < 200$  eV, the  $\tau$  factor attained lower values than  $P(\gamma)$ , which becomes inexact in the range  $T \leq 50$  eV, while for  $T > 200$  eV, the  $\tau$  factor attains larger values than

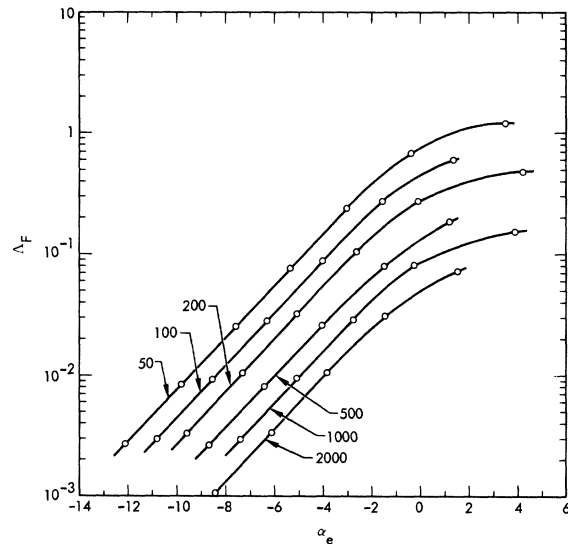


FIG. 9. The plasma-interaction parameter and electron degeneracy  $\alpha_e$  for ionized hydrogen in the range  $50 \leq T \leq 2000$  eV.

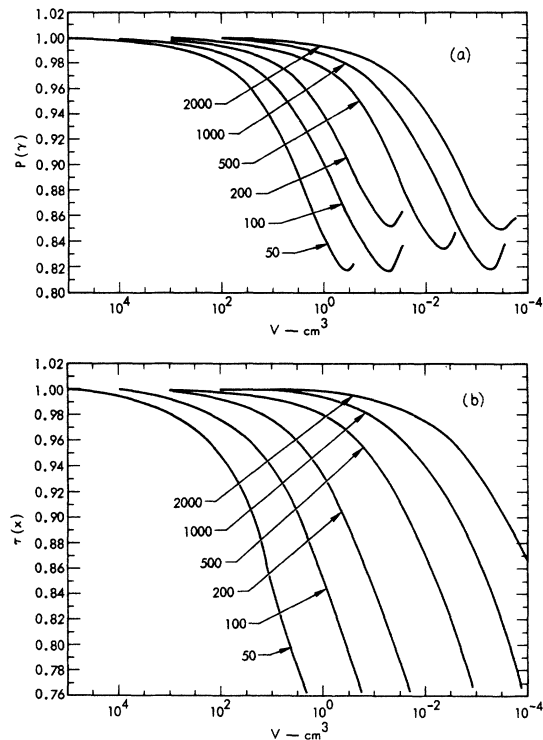


FIG. 10. (a) The wave-mechanical correction  $P(\gamma)$  for ionized hydrogen for  $50 \leq T \leq 2000$  eV. (b) The finite-size correction for the  $\text{H}^+-\text{H}^+$  interaction for  $50 \leq T \leq 2000$  eV.

$P(\gamma)$ . The use of the empirical short-range cutoff in place of the analytical wave-mechanical correction is correct to 5% at worst in the range  $50 \leq T \leq 2000$  eV, and in the range  $100 \leq T \leq 500$  eV, the error is 2% or less. This result indicates that use of the empirical  $\tau(x)$  function to approximate or to continue the wave-mechanical behavior of the ring-sum term in the region where the  $P(\gamma)$  expansion diverges is a reasonable procedure.

A comparison of first- and second-order exchange in the near-classical region is given in Fig. 11. At the lowest temperature, the two terms are nearly equal, because of the near equality of  $\Lambda$  and  $\gamma_e$  at this point. As  $T$  increases, the second-order exchange becomes increasingly less important relative to the first-order term. At  $T > 1000$  eV, it can be neglected for the entire region  $\log_{10} V \leq -3$ . It is clear, however, that if this model is to be carried to higher densities or lower temperatures, both third-order exchange and an exact degeneracy-dependent form of  $S_{2xe}$  must be included. At the lowest volumes plotted for 100 and 200 eV, the classical  $S_{2xe}$  term, if carried up to this point, equals or exceeds the degeneracy-dependent  $S_{1xe}$ . This effect can be removed only by including the Fermi statistics in the second-order term.

The three-rung ladder term has contributed

small but significant effects to the thermodynamic properties at high temperature. The region where  $S_2$  becomes important is at the low-volume end of the isotherms. The comparison between the numerically evaluated  $S_2$  integral and the analytic high-temperature expression of Hoffman and Ebeling<sup>12</sup> is illustrated in Fig. 12. The logarithm of  $|S_2|$  is plotted for electron-electron and ion-ion terms, both negative, and for the electron-ion positive term.

At highest volume, for all three temperatures the agreement between the integral  $S_2$  and asymptotic  $S_2$  is quite good. In all cases, the electron-ion term exhibits the greatest disagreement, which at the largest is 14% at 50 eV and  $10^5 \text{ cm}^3$ . This is due to the ratio  $|\Lambda_{ei}/\gamma_{ei}|$  being smaller than  $\Lambda_{ee}/\gamma_{ee}$ , while  $\Lambda_{ei}$  is negative. This condition,  $\Lambda < 0$  and  $|\Lambda/a|$  large, was shown to be one which produced very rapid changes in  $S_2$ , where the asymptotic expansion starts to diverge. The agreement for the electron-electron term is within a few percent, and for the ion-ion term the two forms agree to four significant figures. As the volume decreases, the two sets of curves begin to separate, until at sufficiently high density, the asymptotic term rapidly diverges from the integral term. In all these cases, this discrepancy grows very rapidly, the electron-electron term diverging first, followed by the electron-ion and then the ion-ion term. About the point where the asymptotic form fails, a stronger curvature sets in for the electron-electron and electron-ion integral terms, denoting the onset of significant electron degeneracy. At the lowest volume points on the isotherms, the electron-electron and electron-ion contributions here begin to decrease, while the ion-ion term still exhibits a classical low-density dependence.

It is of interest to note the partial "cancellation" of the total  $S_2$  term at highest volume. Because of the  $Z^3$  dependence of the three-rung ladder term, the three terms occur in the approximate ratio

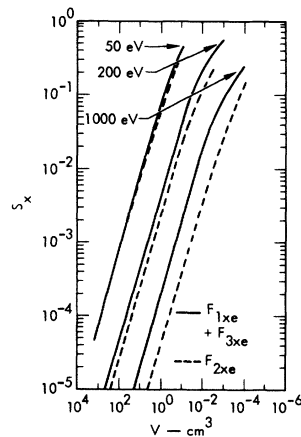


FIG. 11. Exchange free energies for hydrogen. First- plus third-order terms are compared to second order.

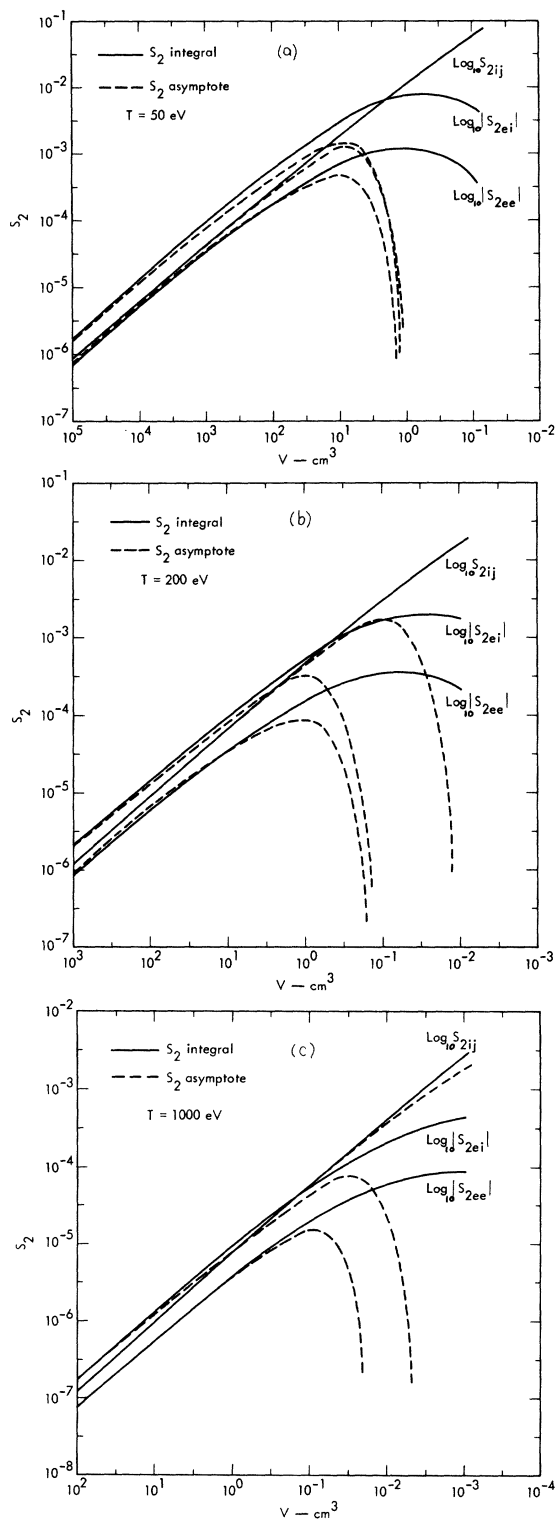


FIG. 12. (a) Three-rung ladder term values for electron-electron, electron-ion, and ion-ion interactions at 50 eV. The integral form agrees closely with the analytic high-temperature asymptotic form for high volume. (b) Three-rung ladder term values at 200 eV. (c) Three-rung ladder term values at 1000 eV.

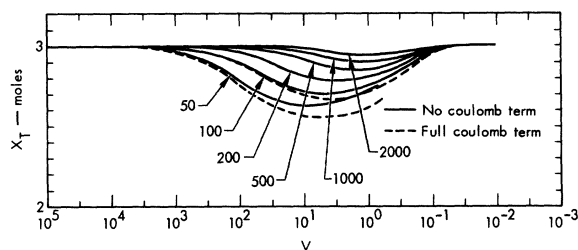


FIG. 13. Ionization equilibrium for helium in the range  $50 \leq T \leq 2000$  eV. The fully ionized plasma contains three moles of particles. At the ionization minimum 50 eV, the  $\text{He}^+$  gas is 63% ionized. The broken lines show the ionization equilibrium with no Coulomb interactions included in the nonideal free-energy model.

(-1, 2, -1), so that their additive effect is about one order of magnitude down from the value of the individual terms. As electron degeneracy begins to affect the electron-electron and electron-ion terms, this approximate equivalence is destroyed, until at lowest volume the total  $S_2$  is closely approximated by the ion-ion term alone.

The full Coulomb configurational free-energy model was also applied to a calculation of the thermodynamic properties of a helium system at high temperature. The thermodynamic effects produced by the Coulomb interaction were similar to those observed in hydrogen, the primary differences being due to the stronger interaction of the doubly charged helium ions. The ionization equilibrium for the  $\text{He}^+-\text{He}^{+2}$  system is shown in Fig. 13 for the temperature range 50–2000 eV. The shift of the ionization minimum toward higher density as the temperature increases is more marked in helium than in hydrogen. The stronger Coulomb interactions (for identical temperature and density) produce larger ionization enhancement in helium, as well as larger Coulomb pressures. In the hydrogen gas, the maximum ionization enhancement produced by the Coulomb effects at 50 eV was 1 part in 400, while for helium at this temperature a 4.2% enhancement is observed.

A comparison of the two dimensionless interaction parameters  $\Lambda_F$  and  $\gamma_{ei}$  is given in Fig. 14 for the two systems. Since the electron density of the two fully ionized gases (for one initial mole of  $\text{H}_2$  and one initial mole of He) is equal for given density and temperature, the electron degeneracy for H and He will be almost equal throughout this strongly ionized high-temperature region. Similarly degeneracy effects will be equivalent. The quantum diffraction parameter, which is related to the wave-mechanical effects in the ring sum and to the first-order exchange, is dependent on the plasma charge:

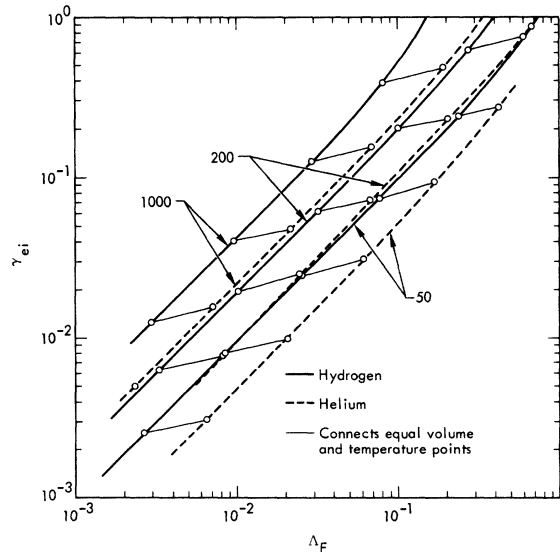


FIG. 14. The plasma-interaction parameter  $\Delta_F$  and quantum diffraction parameter  $\gamma_{ei}$  for hydrogen and helium at 50, 200, and 1000 eV. The connecting lines link points of equal density and temperature for the two gases.

$$\gamma \propto (\sum Z_i^2 x_i)^{1/2}.$$

Hence for helium, at given density and temperature, the  $\gamma$  factors will be  $(6/4)^{1/2}$  or 1.222 times larger than the  $\gamma$  factors for a fully ionized hydrogen gas. Examination of Fig. 14 bears out this relationship, the deviations from this ratio occurring where partial recombination or electron degeneracy are significant. This small  $Z$  dependence indicates that first-order exchange and wave-mechanical effects are less important relative to the direct interaction terms as  $Z$  increases.

The  $Z$  dependence of  $\Lambda$  is given by

$$\Lambda \propto (\sum Z_i^2 x_i / \sum x_i)^{3/2}.$$

For ionized helium, the  $\Lambda$  factors are  $(6/3)^{3/2}$  or 2.828 times the values for ionized hydrogen at the same density and temperature. This relationship is also attained in the results of Fig. 14, slightly modified by recombination and degeneracy effects. This stronger  $Z$  dependence makes the ring term increasingly dominant as  $Z$  increases.

\*Work performed under the auspices of the U. S. Atomic Energy Commission.

<sup>1</sup>H. C. Graboske, Jr., D. J. Harwood, and F. J. Rogers, *Phys. Rev.* **186**, 210 (1969).

<sup>2</sup>E. W. Montroll and J. C. Ward, *Phys. Fluids* **1**, 55 (1958).

<sup>3</sup>E. Meeron, *Phys. Fluids* **1**, 139 (1958).

<sup>4</sup>R. Abe, *Progr. Theoret. Phys. (Kyoto)* **22**, 213 (1959).

<sup>5</sup>H. F. Friedman, *Mol. Phys.* **2**, 23 (1959).

<sup>6</sup>H. E. DeWitt, *J. Nucl. Energy C* **2**, 27 (1961).

<sup>7</sup>H. E. DeWitt, *J. Math. Phys.* **7**, 616 (1966).

<sup>8</sup>D. Bohm and D. Pines, *Phys. Rev.* **82**, 625 (1951).

<sup>9</sup>H. E. DeWitt, *J. Math. Phys.* **3**, 1216 (1962).

<sup>10</sup>H. E. DeWitt, *Low Luminosity Stars*, edited by S. Kumar (Gordon and Breach, New York, 1969).

<sup>11</sup>A. Wasserman, T. J. Buckholtz, and H. E. DeWitt, *J. Math. Phys.* **11**, 477 (1970).

<sup>12</sup>H. J. Hoffmann and W. Ebeling, *Beitr. Plasmaphys.* **8**, 43 (1968).

## Rayleigh Scattering of a Laser Beam from a Massive Relativistic Two-Level Atom<sup>†</sup>

James W. Meyer

*Department of Physics, Purdue University, Lafayette, Indiana 47907*

(Received 8 October 1970)

A relativistic two-level model of a massive atom in the presence of an external plane-wave laser beam is solved. Using the resulting wave functions, the cross sections for the scattering of a photon of the laser frequency or one of its harmonics is calculated. Many interesting nonlinear effects are found, the most striking being the rapid change of the resonance frequency in the cross section for harmonic production as the intensity of the laser is increased. Both approximate and exact numerical results are presented.

### I. INTRODUCTION

The nonlinear interactions of an intense photon (laser) beam with other systems has been the subject of many theoretical investigations. Of particular interest are those that start from first principles, i. e., quantum electrodynamics, since the predictions can then be used as a test of the under-

lying theory. The most investigated subject is nonlinear Compton scattering from a free electron,<sup>1-3</sup> but with present-day lasers the interesting predictions are too small to be measured. In order to increase the size of the nonlinear effects, we would like to study the nonlinear scattering of a photon beam from an atom. For the free electron the only dimensionless parameter available is  $e^2 a^2 / m_e^2$ ,